J. Fluid Mech. (2002), *vol.* 452, *pp.* 361–370. © 2002 Cambridge University Press 361
DOI: 10.1017/S0022112001007091 Printed in the United Kingdom

Scaling of acceleration in locally isotropic turbulence

By **REGINALD J. HILL**

National Oceanic and Atmospheric Administration, Environmental Technology Laboratory, Boulder CO 80305-3328, USA

(Received 28 September 2001 and in revised form 25 October 2001)

The variances of the fluid-particle acceleration and of the pressure-gradient and viscous force are given. The scaling parameters for these variances are velocity statistics measureable with a single-wire anemometer. For both high and low Reynolds numbers, asymptotic scaling formulas are given; these agree quantitatively with DNS data. Thus, the scaling can be presumed known for all Reynolds numbers. Fluid-particle acceleration variance does not obey K41 scaling at any Reynolds number; this is consistent with recent experimental data. The non-dimensional pressure-gradient variance named λ_T/λ_P is shown to be obsolete.

1. Introduction

Accelerations in turbulent flow are violent and are important to many types of studies (La Porta *et al.* 2001). The accelerations discussed here are caused by viscosity, $\nu\nabla_x^2 u_i$, the pressure gradient, $-\partial_{x_i} p$, and the fluid-particle acceleration, a_i, which are related by the Navier–Stokes equation:

$$a_i \equiv \mathrm{D}u_i/\mathrm{D}t = -\partial_{x_i} p + \nu \partial_{x_n}\partial_{x_n} u_i,$$

where $\mathrm{D}u_i/\mathrm{D}t$ denotes the time derivative following the motion of the fluid particle, and u_i is velocity. Here, ν is the kinematic viscosity, $\nabla_x^2 \equiv \partial_{x_n}\partial_{x_n}$ is the Laplacian operator, ∂ denotes differentiation with respect to the subscript variable, summation is implied by repeated indices, p is pressure divided by fluid density; density is constant. Energy dissipation rate per unit mass of fluid is denoted ε.

Kolmogorov's (1941) scaling (K41 scaling) uses ε and ν as parameters, and is based on the assumption that local isotropy is accurate for a given distance r between two points of measurements, $\boldsymbol{x}$ and $\boldsymbol{x}' \equiv \boldsymbol{x} + \boldsymbol{r}$, $r \equiv |\boldsymbol{r}|$. Refinement of K41 to include the effects of turbulence intermittency (Kolmogorov 1962) leads to quantification of the Reynolds number dependence of the deviation from K41 scaling. The choice of Reynolds number was $R_\lambda \equiv u_{rms}\lambda_T/\nu$, based on Taylor's (1935) scale $\lambda_T \equiv u_{rms}/\langle(\partial_{x_1}u_1)^2\rangle^{1/2}$ and $u_{rms} \equiv \langle u_1^2\rangle^{1/2}$, where subscript 1 denotes components along the axis parallel to $\boldsymbol{r}$; also, from $\varepsilon = 15\nu\langle(\partial_{x_1}u_1)^2\rangle$, $R_\lambda = u_{rms}^2/(\varepsilon\nu/15)^{1/2}$. Quantities at $\boldsymbol{x}'$ are denoted u_i', p', and $\Delta u_i \equiv u_i - u_i'$, $\Delta p \equiv p - p'$, etc.

In 1948–1951 (Heisenberg 1948; Obukhov & Yaglom 1951; Batchelor 1951), the pressure-gradient correlation, $\langle\partial_{x_i}p(\boldsymbol{x},t)\partial_{x_j'}p(\boldsymbol{x}',t)\rangle$, mean-squared pressure gradient, $\langle\partial_{x_i}p\partial_{x_i}p\rangle$, and, closely related to those, the pressure structure function, $D_P(r) \equiv \langle(\Delta p)^2\rangle$ were related to the velocity structure function $D_{11}(r) = \langle(\Delta u_1)^2\rangle$ by means of the assumption that u_i and u_i' are joint Gaussian random fields. In fact, the essential approximation, now known to be poor, is that Δu_i must be Gaussian (Hill 1994). One result of that joint Gaussian theory is that pressure-gradient acceleration has as unobservably small effect from intermittency as does D_{11}. In fact, pressure-gradient statistics are strongly affected by intermittency (Hill & Wilczak 1995, hereafter HW; Hill & Thoroddsen 1997, hereafter HT; Hill & Boratav 1997; Vedula & Yeung 1999, hereafter VY; Gotoh & Rogallo 1999, hereafter GR; Gotoh & Fukayama 2001, hereafter GF; Nelkin & Chen 1998; Antonia *et al.* (1999), La Porta *et al.* (2001)).

An advanced theory (HW) relates $D_P(r)$, $\langle \partial_{x_i} p(\boldsymbol{x}, t) \partial_{x'_j} p(\boldsymbol{x}', t) \rangle$, $\langle \partial_{x_i} p \partial_{x_i} p \rangle$, and the pressure spectrum to the fourth-order velocity structure function: $\boldsymbol{D}_{ijkl}(\boldsymbol{r}) \equiv \langle \Delta u_i \Delta u_j \Delta u_k \Delta u_l \rangle$. The theory allows calculation of such pressure-gradient-related statistics from components of $\boldsymbol{D}_{ijkl}$ and therefore by means of hot-wire anemometry, as in HT. This theory is valid for all Reynolds numbers and is based on local isotropy without further assumptions. The degree to which the theory's predictions are accurate must depend on how anisotropic the large scales are and how large the Reynolds number is; isotropy must be approached as Reynolds number becomes small. An advanced theory for the correlation $\langle \nu \nabla_{\boldsymbol{x}}^2 u_i \nu \nabla_{\boldsymbol{x}'}^2 u'_i \rangle$ is given by HT; HT's relationship of this correlation to the third-order velocity structure function $\boldsymbol{D}_{ijk}(\boldsymbol{r}) \equiv \langle \Delta u_i \Delta u_j \Delta u_k \rangle$ has advantages (HT) over the 1948–1951 theory that related $\langle \nu \nabla_{\boldsymbol{x}}^2 u_i \nu \nabla_{\boldsymbol{x}'}^2 u'_i \rangle$ to D_{11}. The advanced theories have been used to compare $D_P(r)$ calculated from $\boldsymbol{D}_{ijkl}(\boldsymbol{r})$ with $D_P(r)$ calculated from DNS pressure fields (figure 1 of Hill & Boratov 1997), as well as the corresponding calculations for $\langle \partial_{x_i} p(\boldsymbol{x}, t) \partial_{x'_j} p(\boldsymbol{x}', t) \rangle$ and $\langle \nu \nabla_{\boldsymbol{x}}^2 u_i \nu \nabla_{\boldsymbol{x}'}^2 u'_i \rangle$ (figures 12, 13 of VY). Since the advanced theories use only the Navier–Stokes equation, incompressibility and local isotropy, comparisons of data with the theory give a measure of the local anisotropy of the data, of numerical limitations, or of inaccuracy of Taylor's hypothesis (when used).

Most studies of turbulent acceleration use the traditional approach of determining the R_λ dependence that results from use of K41 scaling of acceleration statistics [e.g., VY, GR, GF, Antonia *et al.* (1999), La Porta *et al.* (2001)]. The resultant deviation from K41 scaling, i.e. the R_λ dependence, is often called 'anomalous'. There is no anomaly when the advanced theory is employed. Because R_λ contains u_{rms}, it is affected by the large scales where anisotropy is possible, and R_λ is therefore not a parameter of the advanced theory. However, to compare the advanced theory with the existing body of empirical knowledge, the advanced-theory's scales must be expressed in terms of K41 scales, thereby producing dependence on R_λ and ε. However, K41 scaling parameters and R_λ are not the scales within the advanced theory.

2. Scaling of mean-squared pressure gradient

For locally isotropic turbulence, HW gave the relationship between the mean-squared pressure gradient and the fourth-order velocity structure function:

$$\langle \partial_{x_i} p \partial_{x_i} p \rangle = \chi = 4 \int_0^\infty r^{-3} [D_{1111}(r) + D_{\alpha\alpha\alpha\alpha}(r) - 6 D_{11\beta\beta}(r)] \mathrm{d}r, \tag{2.1}$$

where χ is shorthand for the mean-squared pressure gradient for the case of local isotropy. In (2.1), $D_{1111}(r)$, $D_{\alpha\alpha\alpha\alpha}(r)$, and $D_{11\beta\beta}(r)$ are components of $\boldsymbol{D}_{ijkl}(\boldsymbol{r})$; α and β denote the Cartesian axes perpendicular to $\boldsymbol{r}$, and the 1-axis is parallel to $\boldsymbol{r}$. Repeated Greek indices do not imply summation. The result (2.1) applies for all Reynolds numbers and without approximation other than local isotropy.

Defining H_χ as the ratio of the integral in (2.1) to its first term, HW wrote (2.1) as

$$\chi = 4H_\chi \int_0^\infty r^{-3} D_{1111}(r)\mathrm{d}r. \tag{2.2}$$

Equivalently, (2.2) defines H_χ. The purpose of (2.2) as stated in HW is that if the Reynolds number variation of H_χ is known, then (2.2) enables evaluation of χ by calculating the integral in (2.2) using data from a single hot-wire anemometer. Further, HW argued that H_χ is a constant at large Reynolds numbers. VY evaluated H_χ by means of DNS data and found that it is constant at a value of about 0.65 for $80 < R_\lambda < 230$, 230 being their maximum R_λ. Their H_χ only decreased to about 0.55 at $R_\lambda = 20$. Hill (1994) gives $H_\chi \to 0.36$ as $R_\lambda \to 0$ (on the basis that the joint Gaussian assumption can be used in this limit and by use of a formula for the velocity correlation for $R_\lambda \to 0$ given by Batchelor (1956)).

It is useful to express the integral in (2.2) in terms of quantities that have been measured in the past. On the basis of empirical data described in the Appendix, the approximation for high Reynolds numbers is

$$\chi \simeq 3.1 H_\chi \varepsilon^{3/2} \nu^{-1/2} F^{0.79} \simeq 3.9 H_\chi \varepsilon^{3/2} \nu^{-1/2} R_\lambda^{0.25} \quad \text{for} \quad R_\lambda \gtrsim 400, \tag{2.3}$$

where

$$F \equiv \langle (\partial_{x_1} u_1)^4 \rangle / \langle (\partial_{x_1} u_1)^2 \rangle^2$$

is a velocity-derivative flatness. For $H_\chi = 0.65$, (2.3) agrees quantitatively with the DNS data in table 1 of GF for $R_\lambda \geqslant 387$; thereby, the estimated limitation supported in the Appendix, i.e. $R_\lambda \gtrsim 10^3$, seems too conservative. That is why the limitation $R_\lambda \gtrsim 400$ is given in (2.3).

The case of low Reynolds numbers is also given in the Appendix where Taylor's scaling and data from VY are used; the result is

$$\chi \simeq 0.11 \varepsilon^{3/2} \nu^{-1/2} R_\lambda \quad \text{for} \quad R_\lambda \lesssim 20, \tag{2.4}$$

which is shown in figure 1 of VY. Neither (2.4) nor (2.3) is K41 scaling because of their R_λ dependence.

The data of Pearson & Antonia (2001) reveal how the approximation (2.3) is approached as R_λ increases. The inner scale of $D_{1111}(r)$ is denoted by ℓ and is defined in the Appendix as the intersection of viscous- and inertial-range asymptotic formulas for $D_{1111}(r)$. Thus, ℓ is a length scale in the dissipation range. In figures 4 and 5 of Pearson & Antonia (2001), the scaled components of $D_{1111}(r)$ increase most rapidly at $r > \ell$ as R_λ is increased until an inertial range is attained. This implies that the integral in (2.2) will approach the asymptote (2.3) from below. That has been observed, as shown in figure 1, wherein the DNS data of VY and GF are plotted with the asymptotic formulas (2.3) and (2.4); those asymptotes are graphed to $R_\lambda = 100$ and 40, respectively. Because $H_\chi = 0.65$ was used in (2.3) to obtain figure 1, and because VY found $H_\chi \simeq 0.65$ for $80 < R_\lambda < 230$, it appears that H_χ remains constant at about 0.65 for $R_\lambda > 80$. There was no adjustment of (2.3) to cause agreement with the DNS. The agreement is surprising because the empirical data used in the Appendix suggests at least a 15% uncertainty of the coefficients in (2.3). As a reminder of this fortunate circumstance, a $\pm 15\%$ error bar is shown at $R_\lambda = 10^3$ in figure 1. Previously, $\langle \partial_{x_i} p \partial_{x_i} p \rangle / \varepsilon^{3/2} \nu^{-1/2} \propto R_\lambda^{1/2}$ has been reported (VY, GR); this is a good fit to the data of VY in the range $130 < R_\lambda < 300$, and $\langle \partial_{x_i} p \partial_{x_i} p \rangle / \varepsilon^{3/2} \nu^{-1/2} \propto R_\lambda^{0.62}$ is a good fit to the data of GR in the range $39 < R_\lambda < 170$.

In comparison with figure 1, those power laws are local fits over limited ranges

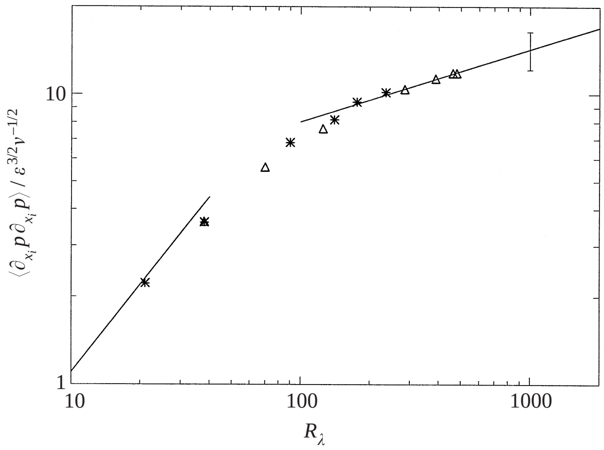

FIGURE 1. K41 scaled mean-squared pressure gradient (sum of squares of the 3 components). $\ast$, VY data; $\triangle$, GF data; ——, equations (2.3), (2.4). 15% error: vertical bar.

of R_λ; they are not asymptotic power laws. On the basis of their equation (59*b*) (of which (2.3) is a refined version), HW gave the first prediction of the increase of $\langle \partial_{x_i} p \partial_{x_i} p \rangle / \varepsilon^{3/2} \nu^{-1/2}$ with Reynolds number. GR noted that (59*b*) gave a weaker dependence on R_λ than their observed $\sim R_\lambda^{1/2}$ dependence, found from DNS for which $R_\lambda < 175$. The reason is now apparent from figure 1: $R_\lambda < 175$ is too low to use (2.3) or (59*b*) of HW. Figure 1 does not support the multifractal result (i.e. $R_\lambda^{0.135}$, about half the slope of (2.3)) given by Borgas (1993).

3. Scaling of $\nu^2 \langle |\nabla_{\boldsymbol{x}}^2 u_i|^2 \rangle$

Derivation of $\nu^2 \langle |\nabla_{\boldsymbol{x}}^2 u_i|^2 \rangle$ from the spatial correlation of $\nu \nabla_{\boldsymbol{x}}^2 u_i$ is given by Hill (2001). It suffices here to state the various equivalent formulas:

$$V_{ii}(0) = \nu^2 \langle |\nabla_{\boldsymbol{x}}^2 u_i|^2 \rangle = 12\nu^2 \langle (\partial_{x_1}^2 u_\beta)^2 \rangle = 35\nu^2 \langle (\partial_{x_1}^2 u_1)^2 \rangle, \tag{3.1}$$

where $\partial_{x_1}^2 \equiv \partial^2 / \partial x_1^2$, and for local stationarity,

$$V_{ii}(0) = \nu \langle \omega_i \omega_j s_{ij} \rangle = -\tfrac{4}{3} \nu \langle s_{ij} s_{jk} s_{ki} \rangle \tag{3.2}$$

$$= -\tfrac{105}{4} \nu \langle (\partial_{x_1} u_\beta)^2 \partial_{x_1} u_1 \rangle = -\tfrac{35}{2} \nu \langle (\partial_{x_1} u_1)^3 \rangle = 0.30 \varepsilon^{3/2} \nu^{-1/2} |S|, \tag{3.3}$$

where ω_i is vorticity and s_{ij} is the rate of strain, and

$$S \equiv \langle (\partial_{x_1} u_1)^3 \rangle / \langle (\partial_{x_1} u_1)^2 \rangle^{3/2}$$

is the velocity-derivative skewness. $|S|$ is known (Sreenivasan & Antonia 1997) to increase with increasing R_λ. Thus, all statistics in (3.1) and (3.2) have the same increase with increasing R_λ when they are non-dimensionalized using K41 scaling. On the other hand, S is approximately constant over the range of about $20 < R_\lambda < 400$ (Sreenivasan & Antonia 1997) such that $V_{ii}(0)$ approximately follows K41 scaling in that range.

The most carefully selected data for S and F at high Reynolds numbers are those of Antonia, Chambers & Satyaprakesh (1981), which are in agreement with data at $R_\lambda = 10^4$ by Kolmyansky, Tsinober & Yorish (2001). The data of Antonia *et al.* (1981) are used for F in (2.3) and give $|S| \simeq 0.5(R_\lambda/400)^{0.11}$ for $R_\lambda > 400$. Substituting

$|S| \simeq 0.5(R_\lambda/400)^{0.11}$ in (3.3) gives

$$V_{ii}(0) \simeq 0.08 R_\lambda^{0.11} \quad \text{for} \quad R_\lambda > 400. \tag{3.4}$$

For $R_\lambda < 20$, Tavoularis, Bennett & Corrsin (1978), Herring & Kerr (1982) and Kerr (1985) show that $|S|$ decreases and does so more rapidly as $R_\lambda \to 0$. The data of Herring & Kerr (1982) suggest that $|S| \simeq R_\lambda/5$ for $R_\lambda < 1$. Although stronger empirical evidence would be helpful, $|S| \simeq R_\lambda/5$ will serve as the asymptotic formula for $R_\lambda < 1$, in which case (3.3) becomes

$$V_{ii}(0) \simeq 0.06\varepsilon^{3/2}\nu^{-1/2}R_\lambda \quad \text{for} \quad R_\lambda < 1. \tag{3.5}$$

4. Scaling of the mean-squared fluid-particle acceleration

For locally isotropic turbulence, the mean-squared fluid-particle acceleration $A_{ii}(0)$ is $\chi + V_{ii}(0)$ because the correlation of $\nabla^2_{x'} u'_i$ and $\partial_{x_j} p$ vanishes by local isotropy (Obukhov & Yaglom 1951). Thus, for any Reynolds number for which local isotropy is valid

$$A_{ii}(0) = 4H_\chi \int_0^\infty r^{-3} D_{1111}(r)\mathrm{d}r - \tfrac{35}{2}\nu\langle(\partial_{x_1}u_1)^3\rangle. \tag{4.1}$$

Therefore, $A_{ii}(0)$ scales with the sum of two terms that behave differently with Reynolds number.

Use of (2.3) and (3.3, 3.4) in (4.1) gives for $R_\lambda \gtrsim 400$,

$$A_{ii}(0) \simeq \varepsilon^{3/2}\nu^{-1/2}(2.0F^{0.79} + 0.3|S|) \simeq \varepsilon^{3/2}\nu^{-1/2}(2.5R_\lambda^{0.25} + 0.08R_\lambda^{0.11}). \tag{4.2}$$

At $R_\lambda = 400$, the term from χ is 70 times greater than the term from $V_{ii}(0)$, and χ increases much faster than $V_{ii}(0)$ for increasing R_λ. The 1948–1951 theory used the joint Gaussian assumption and thereby greatly underestimated $\langle\partial_{x_i}p\partial_{x_i}p\rangle$ (HW, HT). That theory gives equation (3.18) of Obukhov & Yaglom (1951), which is the same as (4.2) except that $1.1|S|^{-1}$ appears in place of $2.0F^{0.79}$. Not only is the magnitude of $1.1|S|^{-1}$ smaller than $2.0F^{0.79}$ by a factor of 5 at $R_\lambda = 400$ but, in addition, $|S|^{-1}$ decreases with further increases of R_λ contrary to the increase of $2.0F^{0.79}$. An empirical result that seems accurate for a variety of flows for $R_\lambda \gtrsim 400$ (Champagne, 1978; Antonia *et al.* 1981) is $|S| = 0.25F^{3/8}$, such that (4.2) can be written as $A_{ii}(0) \simeq \varepsilon^{3/2}\nu^{-1/2}(2.0F^{0.79} + 0.075F^{0.375})$ for $R_\lambda \gtrsim 400$.

For low Reynolds numbers, use of (2.4) in (4.1) gives

$$A_{ii}(0) \simeq \varepsilon^{3/2}\nu^{-1/2}(0.11R_\lambda + 0.3|S|) \quad \text{for} \quad R_\lambda < 20. \tag{4.3}$$

Figure 8 of Herring & Kerr (1982) shows that $0.11R_\lambda > 0.3|S|$ even at their minimum R_λ of 0.5, and that $0.11R_\lambda$ increases rapidly relative to $0.3|S|$ as R_λ increases. Thus, (4.3) shows that the term from χ is the larger contribution to $A_{ii}(0)$ for all R_λ. The behaviour of $A_{ii}(0)$, χ, and $V_{ii}(0)$ for moderate R_λ is shown particularly well in figure 1 of VY.

5. Discussion

5.1. *Obsolescence of* λ_T/λ_P

The length scales $\lambda_P \equiv u_{rms}^2/\langle(\partial_{x_1}p)^2\rangle^{1/2}$ and $\lambda_T \equiv u_{rms}/\langle(\partial_{x_1}u_1)^2\rangle^{1/2}$ were introduced by Taylor (1935) (he included a factor of $\sqrt{2}$ that has historically been dropped from these definitions), and the ratio λ_T/λ_P, and he gave the first evaluation of λ_T/λ_P from turbulent diffusion measurements. $(\lambda_T/\lambda_P)^2 = \langle(\partial_{x_1}p)^2\rangle/[u_{rms}^2\langle(\partial_{x_1}u_1)^2\rangle]$ is a scaled mean-squared pressure gradient; that scaling depends on a large-scale parameter, u_{rms}. As such λ_T/λ_P is not relevant in the advanced theory except in the limit of $R_\lambda \to 0$. Batchelor (1951) obtained, for very large Reynolds numbers $\lambda_T/\lambda_P \propto R_\lambda^{-1/2}$, which is not correct because it is based on the joint Gaussian assumption. By attempting evaluation of λ_T/λ_P, Batchelor (1951) was, in effect, attempting to enable determination of χ from measurements of velocity variance and energy dissipation rate. The advanced theory replaces $(\lambda_T/\lambda_P)^2$ with H_χ. Evaluation of H_χ allows χ to be determined from measurement of a single velocity component and the simple formula (2.2). Figure 3 of GR shows λ_T/λ_P versus R_λ and reveals the following: (i) the strong R_λ dependence of λ_T/λ_P that H_χ does not have; (ii) the deviation of the R_λ dependence of λ_T/λ_P from that predicted by the joint Gaussian assumption (this was also found by VY) and (iii) $R_\lambda < 20$ is required to approach the low-Reynolds-number asymptote. Whereas H_χ depends only on the small scales of turbulence, the dependence of λ_T/λ_P on the large scales via u_{rms} shows that λ_T/λ_P is not relevant in the advanced theory of local isotropy, except in the limit of $R_\lambda \to 0$; for that limit HW shows that $H_\chi \propto (\lambda_T/\lambda_P)^2$.

5.2. *Acceleration data*

Pioneering technology for measuring turbulence accelerations is being developed at Cornell. La Porta *et al.* (2001) report fluid-particle acceleration measured in a cylindrical enclosure containing turbulent water driven by counter-rotating blades. Let 'x' and 'y' denote axes that are transverse and parallel to their cylinder axis, respectively. The acceleration's flatness factor $\langle a_x^4\rangle/\langle a_x^2\rangle^2$ shown in their figure 3 reaches a maximum at $R_\lambda \approx 700$, and is decreased at their next-higher R_λ value, 970, the same is true for their K41-scaled acceleration variances $\langle a_i^2\rangle/\varepsilon^{3/2}\nu^{-1/2}$ in their figure 4, where $i = x$ and y. From (4.2), $A_{ii}(0)/\varepsilon^{3/2}\nu^{-1/2} = 3\langle a_i^2\rangle/\varepsilon^{3/2}\nu^{-1/2}$ is monotonic with R_λ, unlike in figure 4 of La Porta *et al.* (2001). This suggests that the maxima in flatness and variance have the same cause. Their estimates of R_λ and ε both depend on the choice of a velocity component; because the turbulence is anisotropic, the choice of another velocity component will shift their data points along both ordinate and abscissa. This non-universality of their scaling is implied by the disappearance of the maximum in the flatness of $\partial_{x_1}u_1$ as presented by Belin *et al.* (1997) when R_λ is replaced by a universal Reynolds number (Hill, 2001). Belin *et al.* (1997) measure near one counter-rotating blade whereas LaPorta *et al.* (2001) measure in the flow's centre. The two cylinders have different aspect ratios. It is nevertheless instructive to substitute the values of F and $|S|$ measured by Belin *et al.* (1997) into (4.2), divide by 3 to obtain the variance of one component of acceleration, and compare the result with the data of La Porta *et al.* (2001). This is done in figure 2, wherein the data of VY and GF are shown to agree with those of Belin *et al.* (1997). For the Belin *et al.* data, (4.2) produces a maximum similar to that of La Porta *et al.* (2001).

As Belin *et al.* (1997) point out, the maximum in their data for F might be specific to the flow between counter-rotating blades. If so, the same is probably true of La Porta *et al.* (2001) such that their data do not support K41 scaling of acceleration, and therefore do not contradict the advanced theory. Another possibility is that the data of La Porta *et al.* (2001) at $R_\lambda = 970$ is underestimated for unknown reasons. The conclusion suggested by figure 2 and the above uncertainties in interpretation is that the data support the scaling given here and that such important acceleration measurements must continue.

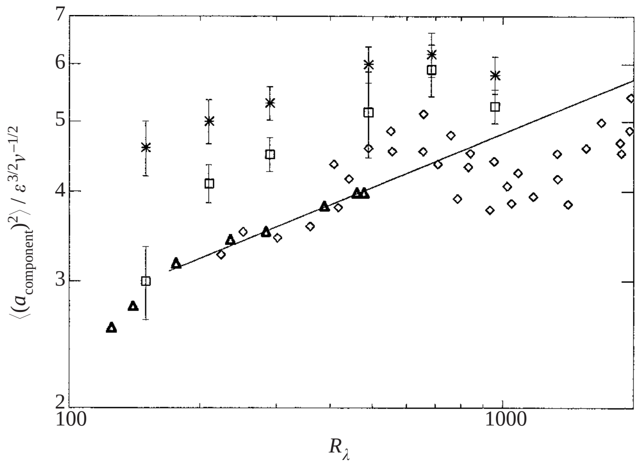

FIGURE 2. K41 scaled mean-squared acceleration component. $\ast$, La Porta *et al.* (2001) data, x-component; □, y-component; ◇, Belin *et al.* (1997) data in equation (4.2); △, combined DNS data of VY and GT; ——, (4.2) divided by 3.

6. Conclusion

The asymptotes (2.3) and (2.4) combined with the DNS data in figure 1 determine $\langle \partial_{x_i} p \partial_{x_i} p \rangle$ for all Reynolds numbers. For all Reynolds numbers the advanced-theory scaling is that $\langle \partial_{x_i} p \partial_{x_i} p \rangle$ scales with the integral in (2.1). For $R_\lambda < 20$, $\langle \partial_{x_i} p \partial_{x_i} p \rangle$ scales with $\varepsilon^{3/2} \nu^{-1/2} R_\lambda$. Because H_χ is apparently constant for $R_\lambda > 80$, $\langle \partial_{x_i} p \partial_{x_i} p \rangle$ scales with $\int_0^\infty r^{-3} D_{1111}(r) \mathrm{d}r$ (i.e. the integral in (2.2)), and $\langle \partial_{x_i} p \partial_{x_i} p \rangle$ scales approximately with $\varepsilon^{3/2} \nu^{-1/2} F^{0.79}$ for $R_\lambda > 400$, and $\varepsilon^{3/2} \nu^{-1/2} F^{0.79}$ is a good approximation when R_λ is as small as 200 (see figure 1). Given that H_χ is constant for $R_\lambda > 80$, $\langle \partial_{x_i} p \partial_{x_i} p \rangle$ could be obtained for $R_\lambda > 80$ using data from a single-wire anemometer by evaluating the integral in (2.2); DNS is not necessary. Using velocity data, it is more accurate to evaluate the integral in (2.2) than its approximation $\varepsilon^{3/2} \nu^{-1/2} F^{0.79}$ because evaluating F requires greater spatial resolution than does evaluation of the integral for the same level of accuracy. Evaluating H_χ from (2.2) using DNS at $R_\lambda > 230$ would be useful.

Now, $V_{ii}(0)$ does scale with any of the derivative moments in (3.1). It does not scale as in the K41 prediction (i.e., $\varepsilon^{3/2} \nu^{-1/2}$) except for those R_λ at which S is constant. The statement in VY that $V_{ii}(0)$ does obey K41 scaling is based on their data, which are within the R_λ range where S is constant.

Fluid-particle acceleration variance, $A_{ii}(0)$, does not scale as in the K41 prediction (i.e. $\varepsilon^{3/2} \nu^{-1/2}$) at large Reynolds numbers because of the factor $(2.5 R_\lambda^{0.25} + 0.08 R_\lambda^{0.11})$ in (4.2). $A_{ii}(0)$ does not approach K41 scaling as $R_\lambda \to 0$ because (3.5) and (4.3) give $A_{ii}(0) \simeq 0.17 \varepsilon^{3/2} \nu^{-1/2} R_\lambda$ for $R_\lambda < 1$. For all Reynolds numbers, fluid-particle acceleration does scale with the sum of velocity statistics that appears on the right-hand side of (4.1).

The advanced theory is devoid of statistics of the large scales. It seems paradoxical that R_λ, which depends on the large scales through u_{rms}, is used above to delineate asymptotic regimes. However, an alternative Reynolds number that depends only on small scales (Hill, 2001) makes the advanced theory self-contained. Use of existing phenomenology caused both ε and R_λ to appear in this paper. However, practical applications result. Turbulent acceleration-induced coalescence of droplets might be key to understanding rain initiation from liquid-water clouds (Shaw & Oncley 2001).

Radar can measure u_{rms} and ε, so $R_\lambda = u_{rms}^2/(\varepsilon\nu/15)^{1/2}$ can be determined; then the three acceleration variances can be determined from equations given here. The present results thereby support radar remote sensing of clouds and cloud microphysical research.

Appendix. High- and low-Reynolds-number asymptotes

A.1. *High-Reynolds-number asymptote*

The lognormal model of Kolmogorov (1962) is used here; the result is found to be insensitive to the intermittency model used. The inertial-range formulas are: $D_{1111}(r) = C'\varepsilon^{4/3}r^qL^{2\mu/9}$, $q = (4/3)-(2\mu/9)$, and $D_{11}(r) = C\varepsilon^{2/3}r^pL^{-\mu/9}$, $p = (2/3)+(\mu/9)$; L is the integral scale; $\mu = 0.25$ is used (Sreenivasan & Kailasnath, 1993), as is $C = 2$ (Sreenivasan 1995). Viscous-range formulas are used: $D_{1111}(r) = \langle(\partial_{x_1}u_1)^4\rangle r^4$ and $D_{11}(r) = \langle(\partial_{x_1}u_1)^2\rangle r^2 = (\varepsilon/15\nu)r^2$. The inner scale of $D_{1111}(r)$, named ℓ, is defined by equating the inertial-range formula with the viscous-range formula at $r = \ell$. In the integrand in (2.2), $D_{1111}(r)$ can be scaled by $D_{1111}(\ell)$ and r by ℓ. Doing so, the integral equals $\frac{3}{2}\ell^2\langle(\partial_{x_1}u_1)^4\rangle$ (HW showed that the remaining dimensionless integral has a value of $\frac{3}{2}$ for large Reynolds numbers; this is based on use of an equation for $D_{1111}(r)$ that is the same as equation (12) in Stolovitzky, Sreenivasan & Juneja (1993), who demonstrate its empirical basis). Next, the otherwise irrelevant Taylor scale λ_T is introduced to make use of published empirical data. The definition of ℓ and the inertial range formulas are used to obtain $(\ell/\eta)^{4-q} = (15C)^2(\lambda_T^2/\eta L)^{2\mu/9}F(\lambda_T)/F$; $F(\lambda_T) \equiv D_{1111}(\lambda_T)/[D_{11}(\lambda_T)]^2$; $F \equiv \langle(\partial_{x_1}u_1)^4\rangle/\langle(\partial_{x_1}u_1)^2\rangle^2$. The essential approximation is that λ_T is in the inertial range (Antonia *et al.* 1982; Pearson & Antonia 2001). Then, $\frac{3}{2}\ell^2\langle(\partial_{x_1}u_1)^4\rangle = \frac{3}{2}C^{4/(4-q)}15^{2(q-2)/(4-q)}[(\lambda_T^2/\eta L)^{2\mu/9}F(\lambda_T)/F]^{2/(4-q)}F\varepsilon^{3/2}\nu^{-1/2}$. For $10^2 < R_\lambda < 5\times10^3$, Zocchi *et al.* (1994) have $\lambda_T^2/L\eta = 30R_\lambda^{-1/2}$ such that $(\lambda_T^2/L\eta)^{(2\mu/9)(2/(4-q))} = (R_\lambda/900)^{-2\mu/[9(4-q)]}$; the exponent of $\lambda_T^2/L\eta$ is about 0.04; so R_λ can vary greatly but $(\lambda_T^2/L\eta)^{0.04}$ remains near unity. The most consistent data for F at high Reynolds numbers are those of Antonia *et al.* (1981), which give $F \simeq 1.36R_\lambda^{0.31}$; the same data (Antonia *et al.* 1982) give $F(\lambda_T) \propto R_\lambda^\mu$ and $F(\lambda_T) \simeq 7.1$ at $R_\lambda = 9400$ so $F(\lambda_T) \simeq 0.72R_\lambda^\mu$. Thus, $\frac{3}{2}\ell^2\langle(\partial_{x_1}u_1)^4\rangle \simeq 0.714R_\lambda^{-0.064}F\varepsilon^{3/2}\nu^{-1/2} = 0.76F^{0.79}\varepsilon^{3/2}\nu^{-1/2} = 0.97R_\lambda^{0.25}\varepsilon^{3/2}\nu^{-1/2}$, i.e.

$$\int_0^\infty r^{-3}D_{1111}(r)\mathrm{d}r \simeq 0.76F^{0.79}\varepsilon^{3/2}\nu^{-1/2} \simeq 0.97R_\lambda^{0.25}\varepsilon^{3/2}\nu^{-1/2}. \tag{A 1}$$

Given that $\mu \approx 0.25$, (A 1) is insensitive of the value of μ and is therefore also insensitive to the choice of intermittency model. Shaw & Oncley (2001) used data from the atmospheric surface layer at $R_\lambda = 1500$ to obtain that (A 1) balances to within the accuracy of their value of F, i.e. about 15%.

The data of Pearson & Antonia (2001) show $D_{\beta\beta\beta\beta}(\lambda_T)/D_{1111}(\lambda_T)$ becoming constant as $R_\lambda \to 10^3$ from below; such a constant value is a reasonable criterion for the integral in (2.1) to be proportional to $\int_0^\infty r^{-3}D_{1111}(r)\mathrm{d}r$ as in (2.2). They show the variation of $D_{1111}(r)$ and $D_{\beta\beta\beta\beta}(r)$ as R_λ varies from 38 to 1200 such that an inertial range appears at the larger R_λ. The above approximation (A 1) requires that the integral in (A 1) approximately converges at its upper limit within the inertial range, for which a reasonable criterion is that there be about one decade of the power law. The data of Pearson & Antonia (2001) show such an extent of the power law as $R_\lambda \simeq 10^3$ is attained. Thus, $R_\lambda \simeq 10^3$ is a well-supported lower bound for the high-Reynolds-number approximation (A 1).

A.2. *Low-Reynolds-number asymptote*

The joint Gaussian assumption is not used here. Taylor's (1935) scaling is used, i.e. scales λ_T and u_{rms} are used when $R_\lambda \to 0$. Taylor's scaling gives $D_{1111}(r) \propto u_{rms}^4$, and that H_χ approaches a constant as $R_\lambda \to 0$. Let $x = r/\lambda_T$. Then (2.2) can be written as $\chi \propto u_{rms}^4 \lambda_T^{-2} \int_0^\infty x^{-3} D_{1111}(x)/u_{rms}^4 \mathrm{d}x$. The dimensionless integral is a number, so $\chi \propto u_{rms}^4 \lambda_T^{-2}$; hence $\chi/(\varepsilon^{3/2}\nu^{-1/2}) \propto R_\lambda$. This behaviour is shown in figure 1 of VY where it appears to become accurate between $R_\lambda = 20$ and 40. In their table II, $\chi/(3\varepsilon^{3/2}\nu^{-1/2}) = 0.74$ at $R_\lambda = 21$. Thus, $\chi = 0.106\varepsilon^{3/2}\nu^{-1/2}R_\lambda$ for $R_\lambda < 20$. Compare 0.106 with the prediction of the joint Gaussian assumption: $6/15^{3/2} = 0.103$ (Hill 1994).

REFERENCES

Antonia, R. A., Bisset, D. K., Orlandi, P. & Pearson, B. R. 1999 Reynolds number dependence of the second-order turbulent pressure structure function. *Phys. Fluids* **11**, 241–243.

Antonia, R. A., Chambers, A. J. & Satyaprakash, B. R. 1981 Reynolds number dependence of high-order moments of the streamwise turbulent velocity derivative. *Boundary-layer Met.* **21**, 159–171.

Antonia, R. A., Satyaprakash, B. R. & Chambers, A. J. 1982 Reynolds number dependence of velocity structure functions in turbulent shear flows. *Phys. Fluids* **25**, 29–37.

Batchelor, G. K. 1951 Pressure fluctuations in isotropic turbulence. *Proc. Camb. Phil. Soc.* **47**, 359–374.

Batchelor, G. K. 1956 *The Theory of Homogeneous Turbulence*. Cambridge University Press.

Belin, F., Maurer, J., Tabeling, P. & Willaime, H. 1997 Velocity gradient distributions in fully developed turbulence: An experimental study. *Phys. Fluids* **9**, 3843–3850.

Borgas, M. S. 1993 The multifractal Lagrangian nature of turbulence. *Phil. Trans. R. Soc. Lond.* A. **342**, 379–411.

Champagne, F. H. 1978 The fine-scale structure of the turbulent velocity field. *J. Fluid Mech.* **86**, 67–108.

Gotoh, T. & Fukayama, D. 2001 Pressure spectrum in homogeneous turbulence. *Phys. Rev. Lett.* **86**, 3775–3778 (referred to herein as GF).

Gotoh, T. & Rogallo, R. S. 1999 Intermittency and scaling of pressure at small scales in forced isotropic turbulence. *J. Fluid Mech.* **396**, 257–285 (referred to herein as GR).

Heisenberg, W. 1948 Zur statistichen theorie der turbulenz. *A. Physik* **124**, 628–657.

Herring, J. R. & Kerr, R. M. 1982 Comparison of direct numerical simulations with predictions of two-point closures for isotropic turbulence convecting a passive scalar. *J. Fluid Mech.* **118**, 205–219.

Hill, R. J. 1994 The assumption of joint Gaussian velocities as applied to the pressure structure function. *NOAA Tech. Rep.* ERL 451-ETL-277 (www.bldrdoc.gov/library).

Hill, R. J. 2001 Alternative to R_λ-scaling of small-scale turbulence statistics. xxx.lanl.gov. physics/0102056.

Hill, R. J. & Boratav, O. N. 1997 Pressure statistics for locally isotropic turbulence. *Phys. Rev. E* **56**, R2363–R2366.

Hill, R. J. & Thoroddsen S. T. 1997 Experimental evaluation of acceleration correlations for locally isotropic turbulence. *Phys. Rev. E* **55**, 1600–1606 (referred to herein as HT).

Hill, R. J. & Wilczak, J. M. 1995 Pressure structure functions and spectra for locally isotropic turbulence. *J. Fluid Mech.* **296**, 247–269 (referred to herein as HW).

Kerr, R. M. 1985 Higher-order derivative correlations and the alignment of small-scale structures in isotropic numerical turbulence. *J. Fluid Mech.* **153**, 31–58.

Kolmogorov, A. N. 1941 The local structure of turbulence in incompressible viscous fluid for very large Reynolds numbers. *Dokl. Akad. Nauk SSSR* **30**, 538–540.

Kolmogorov, A. N. 1962 A refinement of previous hypotheses concerning the local structure of turbulence in a viscous incompressible fluid at high Reynolds number. *J. Fluid Mech.* **13**, 82–85.

Kolmyansky, M., Tsinober, A. & Yorish, S. 2001 Velocity derivatives in the atmospheric surface layer at $Re_\lambda = 10^4$. *Phys. Fluids* **13**, 311–314.

La Porta, A., Voth, G. A., Crawford, A. M., Alexander, A. & Bodenschatz, E. 2001 Fluid particle accelerations in fully developed turbulence. *Nature* **409**, 1017–1019.

Nelkin, M. & Chen, S. 1998 The scaling of pressure in isotropic turbulence. *Phys. Fluids* **10**, 2119–2121.

Obukhov, A. M., & Yaglom, A. M. 1951 The microstructure of turbulent flow. *Prikl. Mat. Mekh.* **15**, 3–26.

Pearson, B. R. & Antonia, R. A. 2001 Reynolds number dependence of turbulent velocity and pressure increments. *J. Fluid Mech.* **444**, 343–382.

Shaw, R. A. & Oncley, S. P. 2001 Acceleration intermittency and enhanced collision kernels in turbulent clouds. *Atmos. Res.* **59/60**, 77–87.

Sreenivasan, K. R. 1995 On the universality of the Kolmogorov constant. *Phys. Fluids* **7**, 2778–2784.

Sreenivasan, K. R. & Antonia, R. A. 1997 The phenomenology of small scale turbulence. *Annu. Rev. Fluid Mech.* **29**, 435–472.

Sreenivasan, K. R. & Kailasnath, P. 1993 An update on the intermittency exponent in turbulence. *Phys. Fluids* A **5**, 512–514.

Stolovitzky, G., Sreenivasan, K. R. & Juneja, A. 1993 Scaling functions and scaling exponents in turbulence. *Phys. Rev.* E **48**, R3217–R3220.

Tavoularis, S., Bennett, J. C. & Corrsin, S. 1978 Velocity-derivative skewness in small Reynolds number, nearly isotropic turbulence. *J. Fluid Mech.* **88**, 63–69.

Taylor, G. I. 1935 Statistical theory of turbulence. *Proc. Roy. Soc. London* **151**, 465–478.

Vedula, P. & Yeung, P. K. 1999 Similarity scaling of acceleration and pressure statistics in numerical simulations of isotropic turbulence. *Phys. Fluids* **11**, 1208–1220 (referred to herein as VY).

Zocchi, G., Tabeling, P., Maurer, J. & Willaime, H. 1994 Measurement of the scaling of the dissipation at high Reynolds numbers. *Phys. Rev.* E **50**, 3693–3700.